RSC Advances

ROYAL SOCIETY OF CHEMISTRY

www.rsc.org/advances

RSC Advances

ARTICLE

Received 00th January 20xx,
Accepted 00th January 20xx

DOI: 10.1039/x0xx00000x

www.rsc.org/

Low loaded palladium nanoparticles on ethylenediamine-functionalized cellulose as an efficient catalyst for electrochemical hydrogen production

Ali Moradpour[a], Ali Ghaffarinejad[*ab], Ali Maleki[c], Vahid Eskandarpour[c] and Ali Motaharian[a]

In this study, for the first time, carbon paste electrode (CPE) was modified with palladium nanoparticles supported on ethylenediamine-functionalized cellulose (PdNPs@EDAC-CPE), and its performance for electrocatalytic hydrogen production was examined. Field emission scanning electron microscopy (FESEM) and energy-dispersive X-ray spectroscopy (EDX) were used to study the morphology and structure of PdNPs@EDAC, respectively. The electrochemical characterizations were performed using cyclic voltammetry (CV), linear sweep voltammetry (LSV), chronoamperometry (CA) and electrochemical impedance spectroscopy (EIS). To optimize conditions, the influence of some parameters including the amounts of PdNPs@EDAC and binder in the electrode composition and the electrolyte type and its pH were examined on the hydrogen production process. Comparison of the proposed electrode with the CPE, CPE modified with functionalized cellulose (EDAC-CPE) and CPE modified with Pd (Pd-CPE) showed that PdNPs@EDAC-CPE has the best performance. The proposed electrode with the very low loaded Pd includes several advantages such as using cellulose as a biodegradable polymer, low cost, very good performance and ease of preparation in a large scale that could be a perfect candidate for high-purity electrocatalytic hydrogen production.

Introduction

Nowadays, the demand for energy is growing and the raw materials for the fossil fuel economy are diminishing. Oil, coal, and natural gas supplies are not replenished as it is consumed. Emissions from fossil fuel usage significantly degrade air quality all over the world and warming up the earth, have signalled the urgent need to find clean, safe and sustainable alternatives to fossil fuels [1]. Hydrogen energy appears to be the one of the most effective solutions and can play a significant role in providing better environment and sustainability [2]. Hydrogen is a renewable energy carrier, and has a high energy yield (122 $kJ.g^{-1}$), which is about 2.75 times greater than hydrocarbon fuels [3]. In nature, hydrogen is always present in bound form, inorganic compounds and water.

There are several methods for hydrogen production including steam reforming [4, 5], gasification [6], thermal catalysis, thermochemical [7], electrolysis[8, 9] hydrolysis [10], photocatalysis [11, 12], and photoelectrocatalytic [13, 14].

Platinum (Pt) is a suitable electrode for the electrochemical production of hydrogen, but it is very expensive and its resource availability is very limited. Therefore, the search for new methods to reduce loaded Pt or replace it with other materials [15, 16] in the hydrogen evolution reaction (HER) has been a topic of current interest. Other metallic electrodes [17] are commonly employ for hydrogen production but they are suffering from corrosion effects and consequently having a short lifetime in acid condition [18]. Carbon paste electrode (CPE) is resistant to corrosion and relatively has a long lifetime in acidic conditions, is inexpensive, and its preparation process is fast [19].

Palladium (Pd) is one of the noble metals. Compared to Pt, Pd has lower cost and is abundant in natural resources. For many years, Pd and its alloys have been known as excellent hydrogen absorbers [20]. Pd and other noble metals are widely investigated as electrode materials for electrocatalytic purposes, e.g. hydrogen production [21-24], catalytic polymerization [25],biosensors [26, 27] and hydrogenation [28]. In addition, it is well known that the physicochemical properties of catalysts are depending heavily on their size, shape and oxidation state. Furthermore, the properties of noble metals could be improved in their nanoparticle sizes.

Cellulose is an organic biopolymer, and has many properties such as, environmentally friendly, high chemical purity, porous structure, biodegradability, large surface area, good hydrophilicity and also low cost [29, 30]. Thus, cellulose could be used as an ideal support for the chemical and electrochemical catalysts[31]. Functionalization of cellulose with a complexing agent such as ethylenediamine could improve the dispersing and stability of Pd nanoparticles (PdNPs) and therefore could improve the electrocatalytic efficiency [30].

[a] Research Laboratory of Real Samples Analysis, Faculty of Chemistry, Iran University of Science and Technology, Tehran 1684613114, Iran.
[b] Electroanalytical Chemistry Research Centre, Iran University of Science and Technology, Tehran 1684613114, Iran.
[c] Catalysts and Organic Synthesis Research Laboratory, Department of Chemistry, Iran University of Science and Technology, Tehran 1684613114, Iran.

Previously, PdNPs loaded on the ethylenediamine-functionalized cellulose (PdNPs@EDAC) have been used as efficient catalyst in the oxidation of hydrazine [30], 1,3-dipolar cycloaddition/direct arylation [32], and Heck and Sonogashira couplings reactions [33]. But, according to our knowledge, there is not any report about the application of this composite as an electrocatalyst for the hydrogen production.

In this study, for the first time, the proposed composite was used to modify the CPE for the electrocatalytic hydrogen production. This electrode has some advantageous such as low cost, high stability, using biodegradable polymer, very good performance and facile preparation.

Experimental

Apparatus and software

Electrochemical studies were accomplished with a potentiostate/galvanostate model of µ-Autolab type II (Echo Chemie, B.V., Netherlands). The electrochemical impedance measurements were done with Autolab PGSTAT 100 (Echo Chemie, B.V., Netherlands). The software of these devices was Nova version 1.7.8. The three-electrode system consisted of CPE or modified CPE as working electrode, Ag|AgCl (3 M KCl) as a reference electrode, and a Pt rod as a counter electrode. The body of the working electrode was a glass tube (3.0 mm i.d.) that was tightly packed with carbon paste. A copper wire inserted into the carbon paste established the electrical contact.

The amount of Pd in the composites was measured by inductively coupled plasma (ICP) model of Shimadzu sequential plasma spectrometer ICPS-7000 Ver.2 (Japan). The morphology of cellulose and its composite with Pd was observed by a Hitachi field emission scanning electron microscopy (FESEM) model F4160 (Japan). The element analysis was carried out by an energy dispersive X-ray analysis (EDX) on a field emission scanning electron microscopy (FESEM/EDX, TESCAN, Mira II LMU, Czech Republic).

Materials and solutions

Graphite fine powder (spectroscopic grade, particle size ≤ 50 µm), sulfuric acid (95-98%), phosphoric acid, cellulose, lithium chloride, dimethylformamide (DMF), benzensulfunyl chloride, ethylendiamine and acetone were obtained from Merck (Germany). Triethylamine (synthesis grade) and palladium catalyst were purchased from Scharlau (Spain) and Riedel-de Haën (Germany), respectively. All of these materials were used without further purification. Deionized water was used for the preparation of solutions.

Synthesis of ethylenediamine-functionalized cellulose

In a typical procedure, a mixture of cellulose (2.00 g) and LiCl (0.05 g) was dispersed in 21.0 mL of DMF. After 10 h stirring at room temperature, 8.0 mmol benzensulfunyl chloride and 0.1 mL triethylamine were added to the mixture, and was vigorously stirred for 24 h at room temperature to afford cellulose benzensulfunate as a white solid powder. Then, without any filtration, 9.0 mL water and 9.0 mmol ethylenediamine were added to the mixture and it was stirred for 20 h at 100 °C. Then, the mixture was cooled down to room temperature and extracted with 60 mL acetone. After filtration, the obtained yellowish white powder was filtered and washed with distilled water and acetone for three times. Finally, the resultant was dried under vacuum at 60 °C.

Synthesis of palladium nanoparticles supported on ethylenediamine-functionalized cellulose

2.00 g dried cellulose functionalized with ethylenediamine (EDAC) was dispersed in 50 mL deionized water and 0.01 g Pd powder was added to the mixture to afford palladium nanoparticles supported on EDAC (PdNPs@EDAC). Then, the mixture was filtered and washed with water for three times.

Preparation of CPE and modified CPE

To prepare CPE, the binder of the carbon paste (n-eicosane) was melted (45–50 °C) and then thoroughly mixed with graphite powder with the ratio of 20:80 to obtain a uniform paste. The paste was packed into the end of the glass tube hole, and then was polished on a smooth paper. It is notable that paraffin is a usual binder in the CPEs [9, 34, 35], but in this study, when paraffin was used, the electrode consolidation was poor.

In order to modify CPE, three modifiers including EDAC, Pd powder and PdNPs@EDAC were used. For the preparation of the modified CPEs, certain amounts of modifier and graphite powder were mixed in a mortar and a certain amount of melted n-eicosane (20%) was added to the mixture. Then, the composition was well mixed to obtain a uniform paste, and the paste was packed at the end of the glass tube hole. Before running any experiment, the surface of the electrodes were polished and smoothed easily on a weighing paper, and then washed with deionized water. For removing H_2 bubbles on the working electrode surface, during all measurements, the electrolyte solution was stirred with a magnet bar beside to the working electrode surface.

Results and discussion

Measurement of Pd loaded on PdNPs@EDAC

PdNPs@EDAC (0.1 g) was added to a mixture of $HCl:HNO_3$ (1:3) (10 mL) and sonicated for 3 h by ultrasonic bath. Then, the mixture was filtered and the total volume of the filtrate was fixed to 25 mL with deionized water, and this solution was analysed with ICP for determination of Pd. The blank solution was prepared with the same procedure for EDAC. The analysis result showed that the Pd loading in PdNPs@EDAC catalyst was 0.425 wt %.

X-ray Analysis

Energy dispersive X-ray analysis (EDX) was used to determine the chemical composition of the PdNPs@EDAC. Fig. 1 shows an EDX picture of this composite. As illustrated in this figure the peaks related to Pd is obviously observed.

Morphology study with SEM

The typical morphologies of the synthesized EDAC and PdNPs@EDAC samples are shown in Fig. 2. Fig. 2 (A) shows FESEM images of functionalized cellulose without palladium nanoparticles (EDAC). In panels B-D, the palladium nanoparticles can be observed clearly on the PdNPs@EDAC, which uniformly dispersed on the cellulose surface with the average particles size below 100 nm.

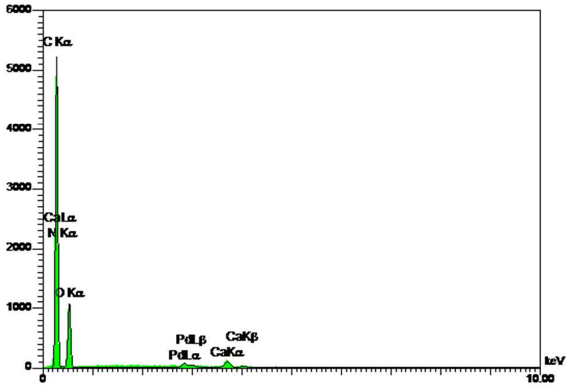

Fig. 1. Energy dispersive spectrum of PdNPs@EDAC

pH effect on HER

pH effect on HER

The effect of pH on the HER was studied with cyclic voltammetry (CV) in the potential range of 1.2 to -1.2 V with the modified CPE containing 25% PdNPs@EDAC and 20% binder. The used solutions were sulfuric acid (1 and 2 M) and phosphate buffer solutions (PBS) with the pHs of 5, 7 and 11. The results of these experiments are illustrated in Fig. 3. In this figure, each voltammogram is the average of three experiments. As shown in Fig. 3, the best result is for 2 M H_2SO_4 with the lowest onset potential (E_i =0.06 V) and the highest current density (j), which may be due to the higher concentration of hydronium ions in the more acidic media. Therefore, 2 M H_2SO_4 was used for the rest of the experiments.

Influence of the amount of modifier on hydrogen production

In this study, PdNPs@EDAC-CPEs with various percent of modifier (5, 10, 15, 20, 25, and 30%) and constant amount of binder (20%) were prepared. The HER on these electrodes were examined by CV in 2 M H_2SO_4 with the scan rate of 100 mV.s^{-1}. Fig. 4 illustrates the average of three cyclic voltammograms. In panel B of this figure a more detail of these voltammograms are illustrated by zooming out on the onset potential region. In this panel the small peaks before rising part of the HER is related to adsorption of hydrogen on the Pd particles. According to this figure the best result is for the 25% PdNPs@EDAC-CPE, which has the lowest E_i (+0.06 V) and the

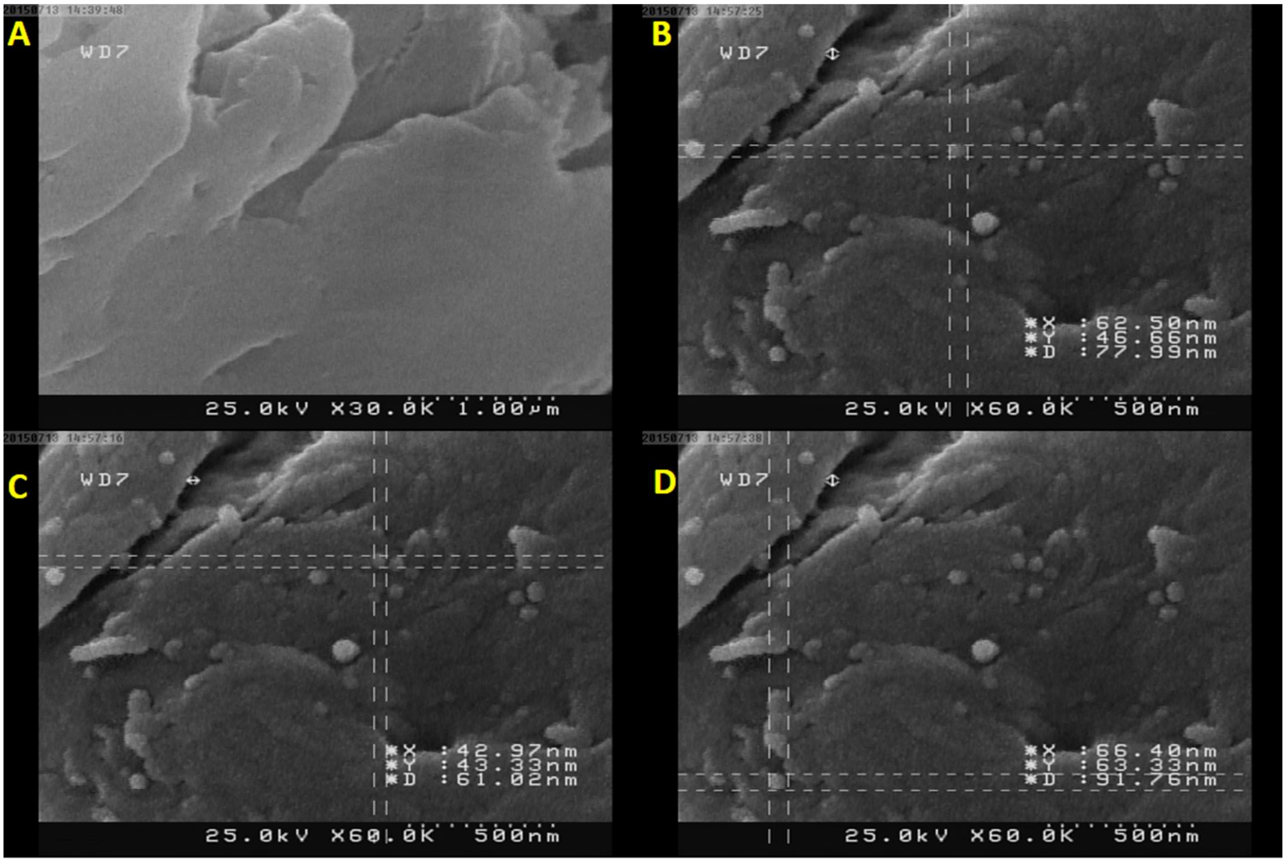

Fig. 2. FESEM images of (A) EDAC and (B-D) PdNPs@EDAC

highest j. Therefore the 25% of PdNPs@EDAC was selected for the rest of experiments. For better comparison Table 1 summarized the E_i and j (at -1.2 V) of these electrodes. The reason of this observation may be related to the increasing of the cellulose portion in the paste, and consequently decreasing the electrode conductivity and increasing IR drop. Therefore as Table 1 shows the overvoltage for HER shift to more negative values and j decreases.

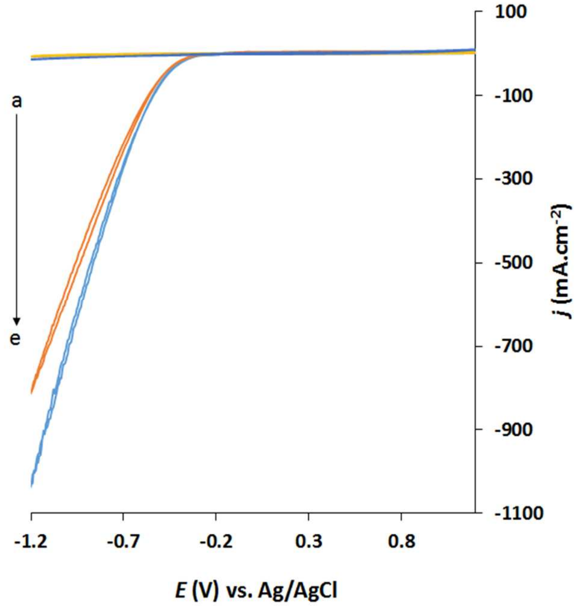

Fig. 3. Cyclic voltammograms of PdNPs@EDAC-CPE with 25% catalyst and 20% binder in PBSs with (a) pH 7, (b) pH 5, (c) pH 11, (d) H_2SO_4 1 M and (e) H_2SO_4 2 M with the scan rate of 100 mV.s^{-1} (each curve is the average of three voltammograms)

Under the optimized conditions of the proposed electrode (PdNPs@EDAC-CPE25%), the same experiments were done for the bare CPE and CPE modified with the equivalent amounts of pure palladium powder (Pd-CPE) based on ICP analysis, and CPE modified with 25% EDAC (EDAC-CPE25%). Fig. 5 illustrates the average of three cyclic voltammograms with the scan rate of 100 mV.s^{-1} in 2 M H_2SO_4 for each of the electrodes. As the figure shows, the presence of Pd improves HER relative to CPE and EDAC-CPE25%.

But, between Pd-CPE and PdNPs@EDAC-CPE25%, which both contain the same amount of Pd, the later has a very better performance. The origin of this observation may be due to the smaller size and more accessibility of the Pd particles on the electrode surface.

Performance study with chronoamperometry

Fig. 6 shows the chronoamperogram of the CPE, EDAC-CPE25%, Pd-CPE and PdNPs@EDAC-CPE25% in 2 M H_2SO_4 with the potential step of -0.8 V for 600 s duration time. Although the presence of Pd in the electrode composition increases the j, the loading of the same amount of Pd on the cellulose improves j value very considerably. In addition, by increasing time the current density on the PdNPs@EDAC-CPE is increased, which means the HER performance increased with time.

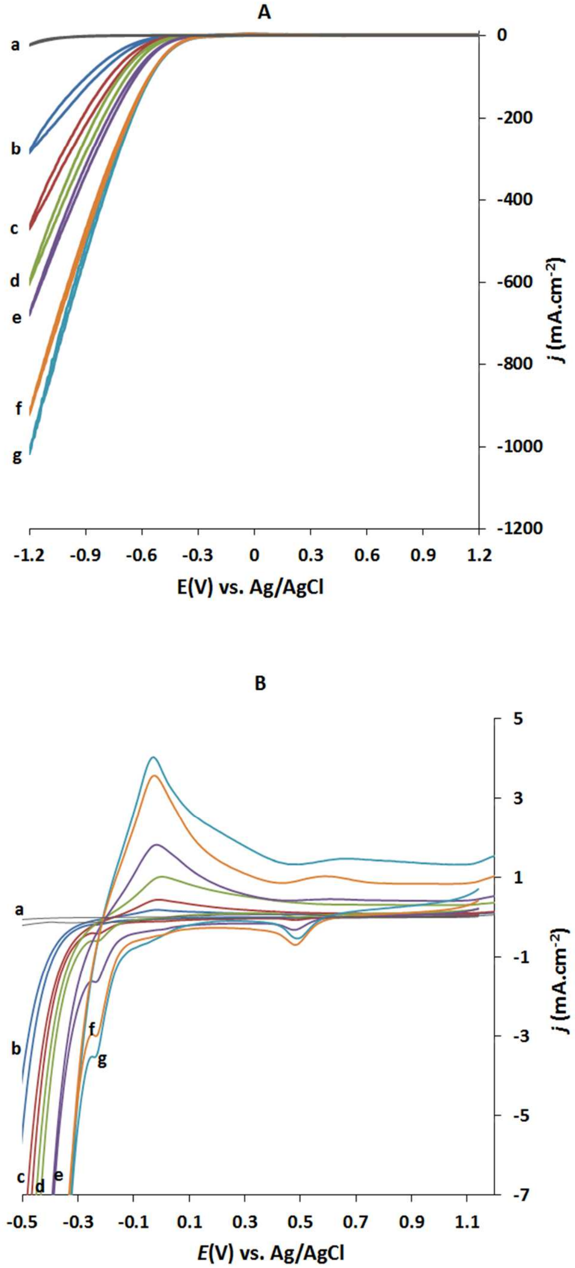

Fig. 4. Panel A: Cyclic Voltammogram of the (a) CPE, (b-g) CPE - PdNPs@EDACs (5, 10, 15, 20, 30, 25% catalyst respectively) in 2 M H_2SO_4 at a scan rate of 100 mV.s^{-1}, and panel B is the zoom out of these CVs at the HER onset potentials.

Steady-state polarization curves for HER on CPE and modified CPEs

Steady-state polarization curves of HER on CPE and modified CPEs were measured by linear sweep voltammetry (LSV) at a

Table 1. Onset potential (E_i) and the current density (j) at -1.2 V for PdNPs@EDAC-CPEs with various modifier amounts (each data is the average of three measurements)

Entry	PdNPs@EDACs (%)	E_i (V)	j (mA.cm^{-2})
1	0	-0.5	-23
2	5	-0.19	-202
3	10	-0.16	-472
4	15	-0.12	-606
5	20	-0.11	-682
6	25	+0.06	-1019
7	30	-0.09	-923

low scan rate (1 mV.s^{-1}) in the potential range of 0.8 to -0.8 V to evaluate their electrocatalytic activities (Fig. 7). At steady-state condition and large cathodic overpotential (η), there was a linear relation between η and log j (Tafel equation),

$$\eta = \frac{2.3\,RT}{\alpha F}\log j_0 - \frac{2.3\,RT}{\alpha F}\log j \qquad \text{(Tafel equation)}$$

Where j_o is the exchange current density, R is the ideal gas constant (8.314 J.mol^{-1}.K^{-1}), T is the absolute temperature and F is the Faraday constant (96485 C.mol^{-1}). The Tafel plots of four electrodes are illustrated in the inset of Fig. 7. The values of Tafel slope (b), j_o and transfer coefficient (α) are summarized in Table 2. Although it is obvious in these voltammograms that the PdNPs@EDAC-CPE25% has the lowest overvoltage and the greatest current density slope, the calculated value of j_o in Table 2 also confirm that the HER kinetic on the proposed electrode is the best.

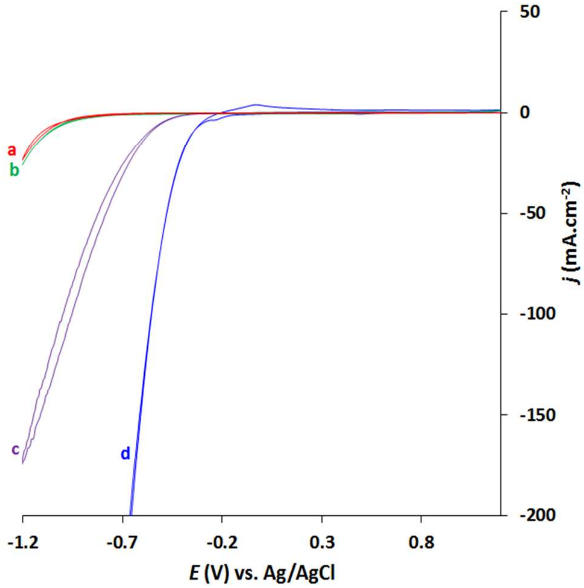

Fig. 5. Comparison of the cyclic voltammograms of the (a) CPE, (b) EDAC-CPE25%, (c) Pd-CPE, and (d) PdNPs@EDAC-CPE25% in 2 M H_2SO_4 with the scan rate of 100 mV.s^{-1} (the curves are the average of three voltammograms)

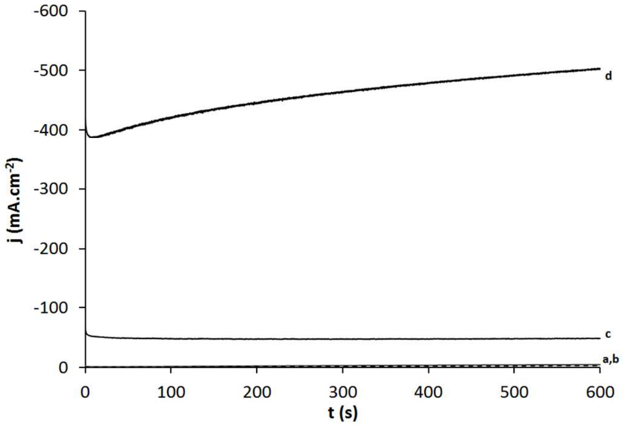

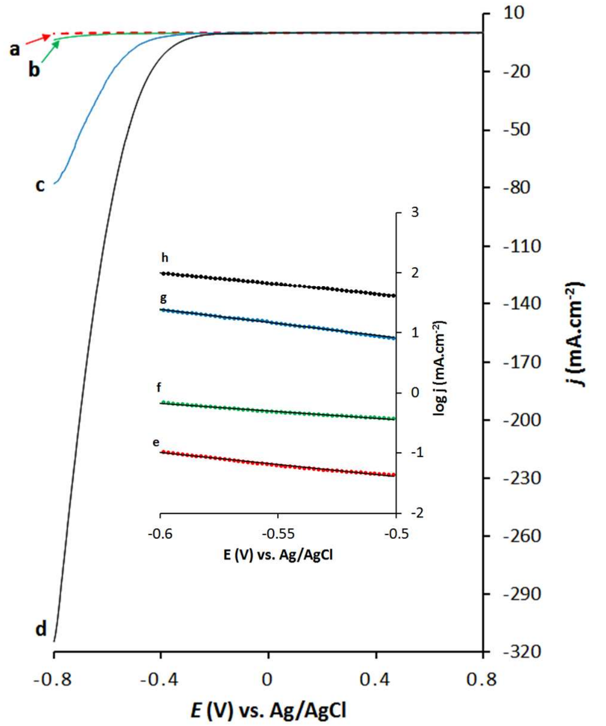

Bode plots for CPE, EDAC-CPE25%, Pd-CPE and frequency range was from 0.01 Hz to 100 kHz. Fig. 9 shows the

Fig. 6. Chronoamperograms with -0.8 V applied potential in 2 M H_2SO_4: (a, dashed line) CPE, (b, solid line) EDAC-CPE25%, (c) Pd-CPE and (d) PdNPs@EDAC-CPE25%.

Fig. 7. Steady-state polarization curves (scan rate 1 mV.s^{-1}) of: (a, dashed line) HER on CPE, (b, solid line) EDAC-CPE25%, (c) Pd-CPE, (d) PdNPs@EDAC-CPE25%; Inset: Tafel plots for (e) CPE, (f) EDAC-CPE25%, (g) Pd-CPE, (h) PdNPs@EDAC-CPE25%.

Table 2. Tafel slopes (b), exchange current densities (j_o) and transfer coefficients (α) for HER on CPE and modified CPEs

Electrode	j_o (mA.cm^{-2})	b (mV.dec^{-1})	α
CPE	1.64×10^{-8}	249	0.24
EDAC-CPE25%	7.13×10^{-5}	367	0.16
Pd-CPE	4.70×10^{-4}	212	0.28
PdNPs@EDAC-CPE25%	1.52×10^{-1}	254	0.23

Electrochemical impedance analysis

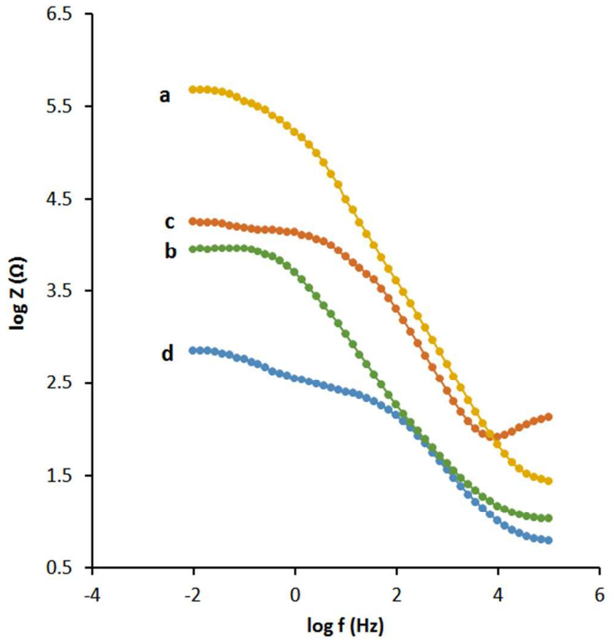

Fig. 8. Bode plots in 2 M H_2SO_4 at the frequency range of 0.01 Hz – 100 kHz. (a) CPE, (b) CPE-EDAC25%, (c) Pd-CPE and (d) PdNPs@EDAC-CPE25

The electrochemical impedance spectroscopy (EIS) measurements were carried out to study the electrode/electrolyte interface and to investigate the HER. The measurements were carried out in 2 M H_2SO_4 and at -0.2 V. The frequency range was from 0.01 Hz to 100 kHz. Fig. 8 shows the Bode plots for CPE, EDAC-CPE25%, Pd-CPE and PdNPs@EDAC-CPE25%. For Pd-CPE and PdNPs@EDAC-CPE25% two step wave is observed, which are related to charge transfer resistance (R_p) and hydrogen adsorption resistance (R_{ad})[21]. As observed in this figure, the total wave height for these electrodes is as this order: CPE > CPE - EDAC25%>Pd-CPE>PdNPs@EDAC-CPE25%.

According to the inverse relation between the wave height and the kinetic of charge transfer, it can be concluded that the better HER efficiency is for PdNPs@EDAC-CPE25%, which is in agreement with the previous observations.

Conclusion

In summary, for the first time, Pd nanoparticles were loaded on the ethylenediamine-functionalized cellulose, and this composite was used as an electrocatalyst for HER. The catalyst characteristics and its morphology were studied with XRD, FT-IR and SEM analyses. The effect of important parameters including pH, electrolyte type and the catalyst amount in the electrode composition on HER performance was evaluated. In comparison with CPE, Pd-CPE and EDAC-CPE25%, the proposed electrode has the best efficiency for HER. The main advantage of this electrode is its high performance with the very low loaded Pd in the electrode composition. According to simplicity, ease of preparation, using cellulose as a biodegradable polymer and low cost, this modified electrode can be used for efficient hydrogen production.

Acknowledgement

We gratefully acknowledge the partial support of this work from the Research Council of the Iran University of Science and Technology.

Notes and references

1 M. Wang, L. Chen and L. Sun, *Energy Environ. Sci.*, 2012, **5**, 6763-6778.
2 I. Dincer, *Int. J. Hydrogen Energy.*, 2012, 37, 1954-1971.
3 M. F. Arooj, S.-K. Han, S.-H. Kim, D.-H. Kim and H.-S. Shin, *Int. J. Hydrogen Energy*, 2008, **33**, 3289-3294.
4 A. Haryanto, S. Fernando, N. Murali and S. Adhikari, *Energy Fuels*, 2005, **19**, 2098-2106.
5 A. Romero, M. Jobbágy, M. Laborde, G. Baronetti and N. Amadeo, *Appl. Catal.*, 2014, **470**, 398-404.
6 G. J. Stiegel and M. Ramezan, *Int. J. Coal Geol.* , 2006, **65**, 173-190.
7 G. F. Naterer, S. Suppiah, L. Stolberg, M. Lewis, Z. Wang, V. Daggupati, K. Gabriel, I. Dincer, M. A. Rosen, P. Spekkens, S. N. Lvov, M. Fowler, P. Tremaine, J. Mostaghimi, E. B. Easton, L. Trevani, G. Rizvi, B. M. Ikeda, M. H. Kaye, L. Lu, I. Pioro, W. R. Smith, E. Secnik, J. Jiang and J. Avsec, *Int. J. Hydrogen Energy.*, 2010, **35**, 10905-10926.
8 M. Wang, Z. Wang, X. Gong and Z. Guo, *Renewable and Sustainable Energy Rev.*, 2014, **29**, 573-588.
9 A. Ghaffarinejad, N. Sadeghi, H. Kazemi, A. Khajehzadeh, M. Amiri and A. Noori, *J. Electroanal. Chem.*, 2012, **685**, 103-108.
10 T. T. Vu, T. Valdés-Solís and G. Marbán, *Appl. Catal.*, B. , 2014, **160**, 57-66.
11 X. Zong, Z. Xing, H. Yu, Y. Bai, G. Q. M. Lu and L. Wang, *J. Catal.* , 2014, **310**, 51-56.
12 T. S. Teets and D. G. Nocera, *Chem. Commun.*, 2011, **47**, 9268-9274.
13 S. Ichikawa and R. Doi, *Thin Solid Films*, 1997, **292**, 130-134.
14 M. Ye, J. Gong, Y. Lai, C. Lin and Z. Lin, *J. Am. Chem. Soc.*, 2012, **134**, 15720-15723.
15 D. Merki, S. Fierro, H. Vrubel and X. Hu, *Chem. Sci.*, 2011, **2**, 1262-1267.
16 P.-A. Jacques, V. Artero, J. Pécaut and M. Fontecave, *Proceedings of the National Academy of Sciences*, 2009, **106**, 20627-20632.
17 G. A. Felton, R. S. Glass, D. L. Lichtenberger and D. H. Evans, *Inorg.Chem.*, 2006, **45**, 9181-9184.
18 A. Abbaspour and E. Mirahmadi, *Fuel*, 2013, **104**, 575-582.
19 I. Švancara, K. Vytřas, K. Kalcher, A. Walcarius and J. Wang, *Electroanalysis*, 2009, **21**, 7-28.
20 M. Łukaszewski, T. Kędra and A. Czerwiński, *Electrochim. Acta.*, 2010, **55**, 1150-1159.
21 A. Safavi, S. H. Kazemi and H. Kazemi, *Fuel*, 2014, **118**, 156-162.
22 F. A. Al-Odail, A. Anastasopoulos and B. E. Hayden, *Top. Catal.*, 2011, **54**, 77-82.
23 Y.-X. Huang, X.-W. Liu, X.-F. Sun, G.-P. Sheng, Y.-Y. Zhang, G.-M. Yan, S.-G. Wang, A.-W. Xu and H.-Q. Yu, *Int. J. Hydrogen Energy*, 2011, **36**, 2773-2776.

24 M. Luo, W. Yao, C. Huang, Q. Wu and Q. Xu, *RSC Adv.*, 2015, **5**, 40892-40898.
25 J. Yuan, J. Zhao, F. Song, W. Xu, Y. Mu, J. Chen and Z. Zhang, *Appl. Organomet.*, 2014, **28**, 484-494.
26 L.-M. Lu, H.-B. Li, F. Qu, X.-B. Zhang, G.-L. Shen and R.-Q. Yu, *Biosens. Bioelectron.*, 2011, **26**, 3500-3504.
27 H. Bai, M. Han, Y. Du, J. Bao and Z. Dai, *Chem. Commun.*, 2010, **46**, 1739-1741.
28 S. Kidambi and M. L. Bruening, *Chem. Mater.*, 2005, **17**, 301-307.
29 H. Huang, P. He, N. Hu and Y. Zeng, *Bioelectrochemistry*, 2003, **61**, 29-38.
30 H. Ahmar, S. Keshipour, H. Hosseini, A. R. Fakhari, A. Shaabani and A. Bagheri, *J. Electroanal. Chem.*, 2013, **690**, 96-103.
31 R. Patel, J. Barad, S. Nandanwar, A. Dabbawala, M. Chakraborty, P. Parikh and H. Baja, *Kinet. Catal.*, 2015, **56**, 173-180.
32 S. Keshipour and A. Shaabani, *Appl. Organomet. Chem.*, 2014, **28**, 116-119.
33 S. Keshipour, S. Shojaei and A. Shaabani, *Cellulose*, 2013, **20**, 973-980.
34 A. Ghaffarinejad, F. Hashemi, Z. Nodehi and R. Salahandish, *Bioelectrochemistry*, 2014, **99**, 53-56.
35 A. Ghaffarinejad, E. Magsoudi and N. Sadeghi, *Anal. Bioanal. Electrochem.*, 2013, 5,316-324.